# On the switching-induced dc-link voltage ripple in three-level converters with a neutral point

Ioannis Tsoumas
ABB System Drives
Austrasse
5300 Turgi, Switzerland
E-Mail: ioannis.tsoumas@ch.abb.com

Tobias Geyer
ABB System Drives
Austrasse
5300 Turgi, Switzerland
E-Mail: tobias.geyer@ch.abb.com

## Keywords

«Voltage Source Converter», «Pulse Width Modulation», «Harmonics».

## Abstract

The operation of a three-level (3L) converter with a neutral point (NP) employed in a medium voltage (MV) wind energy conversion system (WECS) is investigated. In particular, the voltage ripple of the upper or the lower half of the dc-link and its dependence on the relative phase of the carriers in a carrier-based pulse width modulation (CB-PWM) scheme is investigated. It is shown that the carrier phase has no influence on the half dc-link voltage ripple.

## Introduction

The peak value of the voltage of each half of the dc-link is an important design related quantity of a 3L converter with a neutral point, because its value must not exceed the maximum blocking voltage of the semiconductors. When carrier-based pulse width modulation (CB-PWM) is employed for the converter modulation the ripple of the above voltage can be separated in two groups of frequency components: low frequency components related to the average value of the output voltage within one switching period (switching is not taken into account) [1] and high frequency components related to the switching. The former depend on the CB-PWM reference and the current displacement factor and they have been examined in detail in previous works [1]-[3], where a special CB-PWM reference to suppress the low frequency ripple has been derived.

In this work we focus on the latter, the frequency components related to the switching. Exact knowledge of the characteristics of the above components is of paramount importance, since they contribute to the peak value of half the dc-link voltage. Knowledge of their dependence on the CB-PWM reference and the carrier configuration, as well as on the modulation index and the current displacement factor is necessary for a correct selection of the dc-link capacitance value.

## Mathematical modelling of the converter

The circuit diagram of a 3L voltage source converter with an NP is shown in Fig. 1. The dc-link capacitances $C$ are considered identical but the instantaneous voltages of the upper and lower dc-link halves, $v_{\mathrm{dc,h}}(t)$ and $v_{\mathrm{dc,l}}(t)$, may be different. The integer variable $u_x \in \{-1,0,1\}$ denotes the switch position in the phase leg $x$, with $x \in \{\mathrm{a},\mathrm{b},\mathrm{c}\}$. The variable will henceforth be referred to as switching function. The voltages of the three phases referred to the NP for different values of the switching function are given by

$$v_x(t) = \begin{cases} v_{\mathrm{dc,h}}(t), & u_x(t) = 1 \\ 0, & u_x(t) = 0 \\ v_{\mathrm{dc,l}}(t), & u_x(t) = -1 \end{cases} . \tag{1}$$

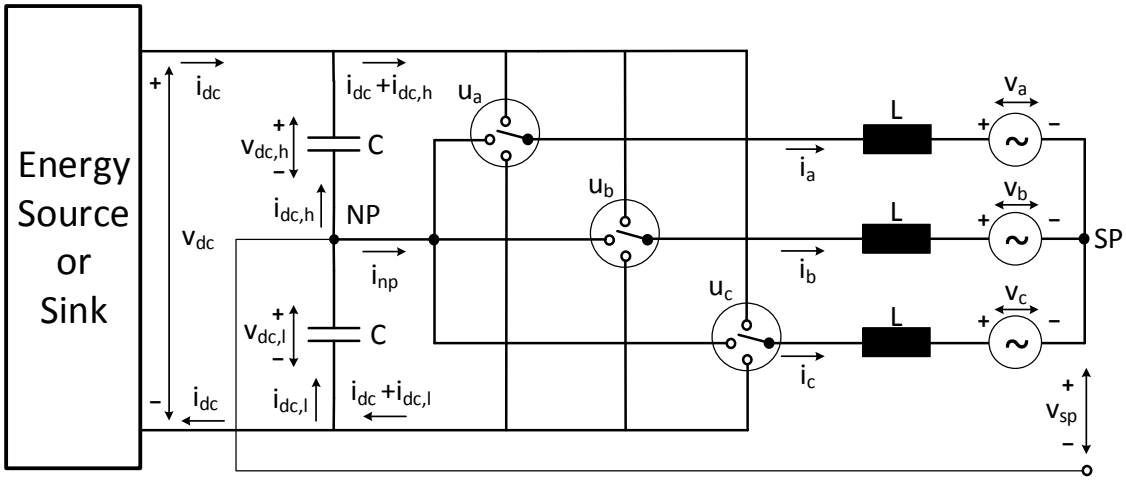

Fig. 1: Circuit diagram of a 3L voltage source converter with a neutral point and ideal switches supplying a 3-phase AC system [4].

The total instantaneous dc-link voltage is given by

$$v_{\mathrm{dc}}(t) = v_{\mathrm{dc,h}}(t) + v_{\mathrm{dc,l}}(t) \tag{2}$$

and the NP potential by

$$v_{\mathrm{np}}(t) = \frac{1}{2}\left[v_{\mathrm{dc,l}}(t) - v_{\mathrm{dc,h}}(t)\right] . \tag{3}$$

The NP potential evolves as a function of the NP current $i_{\mathrm{np}}(t)$ according to

$$\frac{\mathrm{d}v_{\mathrm{np}}}{\mathrm{d}t} = \frac{1}{2}\left[\frac{\mathrm{d}v_{\mathrm{dc,l}}(t)}{\mathrm{d}t} - \frac{\mathrm{d}v_{\mathrm{dc,h}}(t)}{\mathrm{d}t}\right] = -\frac{1}{2}\left[\frac{1}{C}i_{\mathrm{dc,l}}(t) - \frac{1}{C}i_{\mathrm{dc,h}}(t)\right] =$$

$$-\frac{1}{2C}\left[i_{\mathrm{dc,l}}(t) - i_{\mathrm{dc,h}}(t)\right] = -\frac{1}{2C}i_{\mathrm{np}}(t) ,$$

which leads to

$$v_{\mathrm{np}}(t) = -\frac{1}{2C}\int_0^t i_{\mathrm{np}}(\tau)\mathrm{d}\tau + v_{\mathrm{np}}(0). \tag{4}$$

To calculate $v_{\mathrm{np}}$ as a function of the angle in (4) we make a change of variable from $t$ to $\theta = \omega t$

$$v_{\mathrm{np}}(\theta) = -\frac{1}{2\omega C}\int_0^\theta i_{\mathrm{np}}(\zeta)\mathrm{d}\zeta + v_{\mathrm{np}}(0) .$$

The NP current can be calculated from the AC currents as follows:

$$i_{\mathrm{np}}(t) = \sum_{x\in\{\mathrm{a,b,c}\}} (1 - |u_x(t)|)\, i_{\mathrm{x}}(t), \quad \text{with } x \in \{\mathrm{a,b,c}\}. \tag{5}$$

If $\sum_{x\in\{\mathrm{a,b,c}\}} i_{\mathrm{x}}(t) = 0$ (star connection of the phases or symmetrical currents) we get from (5)

$$i_{\mathrm{np}}(t) = -\sum_{x\in\{\mathrm{a,b,c}\}} |u_x(t)| i_x(t) . \tag{6}$$

The phase currents appear on the upper and the lower rail of the dc-link if the corresponding switching function $u_x$ is equal to 1 and $-1$ respectively. Thus, they can be modelled as follows [4]:

$$i_{\mathrm{dc}}(t) + i_{\mathrm{dc,h}}(t) = \sum_{x\in\{\mathrm{a,b,c}\}} u_x(t)\frac{u_x(t)+1}{2} i_x(t) =$$

$$\frac{1}{2}\sum_{x\in\{\mathrm{a,b,c}\}} |u_x(t)| i_x(t) + \frac{1}{2}\sum_{x\in\{\mathrm{a,b,c}\}} u_x(t) i_x(t) \tag{7.a}$$

and

$$i_{\mathrm{dc}}(t)+i_{\mathrm{dc,l}}(t) = -\sum_{x\in\{\mathrm{a,b,c}\}} u_x(t)\frac{u_x(t)-1}{2} i_x(t) = -\frac{1}{2}\sum_{x\in\{\mathrm{a,b,c}\}} |u_x(t)| i_x(t) + \frac{1}{2}\sum_{x\in\{\mathrm{a,b,c}\}} u_x(t) i_x(t). \quad (7.b)$$

If we subtract $i_{\mathrm{dc}}$ from the above currents, the currents in the dc-link capacitors can be calculated:

$$i_{\mathrm{dc,h}}(t) = \frac{1}{2}\sum_{x\in\{\mathrm{a,b,c}\}} u_x(t) i_x(t) + \frac{1}{2}\sum_{x\in\{\mathrm{a,b,c}\}} |u_x(t)| i_x(t) - i_{\mathrm{dc}}(t) \quad \text{and} \quad (8.a)$$

$$i_{\mathrm{dc,l}}(t) = \frac{1}{2}\sum_{x\in\{\mathrm{a,b,c}\}} u_x(t) i_x(t) - \frac{1}{2}\sum_{x\in\{\mathrm{a,b,c}\}} |u_x(t)| i_x(t) - i_{\mathrm{dc}}(t)\ . \quad (8.b)$$

The capacitor voltages are given by

$$v_{\mathrm{dc,h}}(t) = -\frac{1}{C}\int_0^t i_{\mathrm{dc,h}}(\tau)d\tau + v_{\mathrm{dc,h}}(0) =>$$

$$v_{\mathrm{dc,h}}(\theta) = -\frac{1}{\omega C}\int_0^\theta \left[\frac{1}{2}\sum_{x\in\{\mathrm{a,b,c}\}} |u_x(\zeta)| i_x(\zeta) + \frac{1}{2}\sum_{x\in\{\mathrm{a,b,c}\}} u_x(\zeta) i_x(\zeta) - i_{\mathrm{dc}}(\zeta)\right] d\zeta + v_{\mathrm{dc,h}}(0) \quad (9.a)$$

and

$$v_{\mathrm{dc,l}}(t) = -\frac{1}{C}\int_0^t i_{\mathrm{dc,l}}(\tau)d\tau =>$$

$$v_{\mathrm{dc,l}}(\theta) = -\frac{1}{\omega C}\int_0^\theta \left[-\frac{1}{2}\sum_{x\in\{\mathrm{a,b,c}\}} |u_x(\zeta)| i_x(\zeta) + \frac{1}{2}\sum_{x\in\{\mathrm{a,b,c}\}} u_x(\zeta) i_x(\zeta) - i_{\mathrm{dc}}(\zeta)\right] d\zeta + v_{\mathrm{dc,l}}(0). \quad (9.b)$$

Finally, from (2) and (9) the total dc-link voltage can be calculated:

$$v_{\mathrm{dc}}(t) = v_{\mathrm{dc,h}}(t) + v_{dc,\mathrm{l}}(t) =>$$

$$v_{\mathrm{dc}}(\theta) = \frac{1}{\omega C}\int_0^\theta \left[-\sum_{x\in\{\mathrm{a,b,c}\}} u_x(\zeta) i_x(\zeta) + 2 i_{\mathrm{dc}}(\zeta)\right] \mathrm{d}\zeta + v_{\mathrm{dc}}(0)\ . \quad (10)$$

By reformulating (2) and (3) the capacitor voltages can be also expressed as

$$v_{\mathrm{dc,h}}(t) = \frac{v_{\mathrm{dc}}(t)}{2} - v_{\mathrm{np}}(t)\ , \quad (11.a)$$

$$v_{\mathrm{dc,l}}(t) = \frac{v_{\mathrm{dc}}(t)}{2} + v_{\mathrm{np}}(t)\ . \quad (11.b)$$

As can be seen from (11) the voltage of each half of the dc-link is equal to the sum or the difference of half the total dc-link voltage and the NP potential.

## Harmonics of the switching function

The switching that takes place in a 3L converter generates harmonic components at multiples of the carrier frequency and at their respective sidebands. The two carriers can be arranged either in phase disposition (PD) or in phase opposition-disposition (POD). With PD the two level-shifted carriers are in phase, whereas with POD the carriers have a phase difference of $\pi$. Analytical solutions of the switching function harmonics caused by modulation have been calculated in [5] for both cases when a sinusoidal reference is considered for the CB-PWM.

In the case of PD the switching function in phase a can be expressed as the following sum of harmonics:

$$u_{\mathrm{a}} = \sum_{m\epsilon\mathbb{N}} \frac{1}{2m-1} \mathrm{C}_{2m-1} \cos[(2m-1)\omega_c t] + \frac{2}{\pi}\sum_{m\epsilon\mathbb{N}} \frac{1}{2m} \sum_{n\epsilon\mathbb{Z}} \mathrm{C}_{2m,2n+1} \cos[2m\omega_c t + (2n+1)\omega_1 t] + \frac{8}{\pi^2}\sum_{m\epsilon\mathbb{N}} \frac{1}{2m-1} \sum_{n\epsilon\mathbb{Z}\setminus\{0\}} \mathrm{C}_{2m-1,2n} \cos[(2m-1)\omega_c t + 2n\omega_1 t], \quad (12)$$

where $\omega_c$ is the carrier angular frequency and $\omega_1$ is the fundamental angular frequency. The coefficients $\mathrm{C}_{2m-1}$, $\mathrm{C}_{2m,2n+1}$, $\mathrm{C}_{2m-1,2n}$, have been analytically calculated for a sinusoidal reference and natural sampling in [5], but not for a reference that includes a CM component. As it will become evident from the subsequent numerical analysis the coefficients $\mathrm{C}_{2m-1}$, $\mathrm{C}_{2m,2n+1}$, $\mathrm{C}_{2m-1,2n}$ depend on the modulation index. The latter is defined by the ratio of the amplitude of the fundamental harmonic to half the dc-link voltage:

$$m_{3\mathrm{L}} = \frac{\hat{v}_{\mathrm{a1}}}{v_{\mathrm{dc}}/2} \quad (13)$$

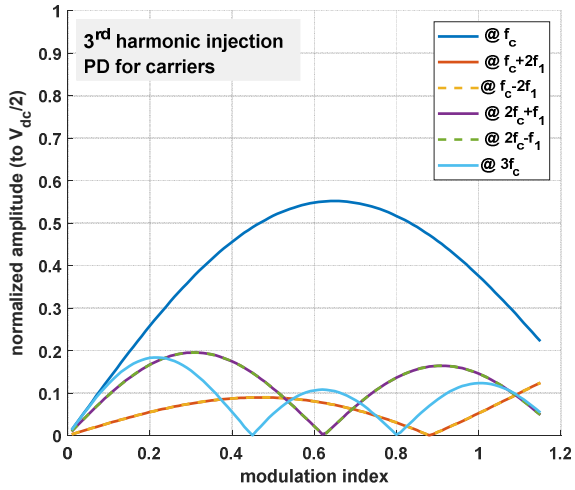


Fig. 2: Switching function harmonics for PD.

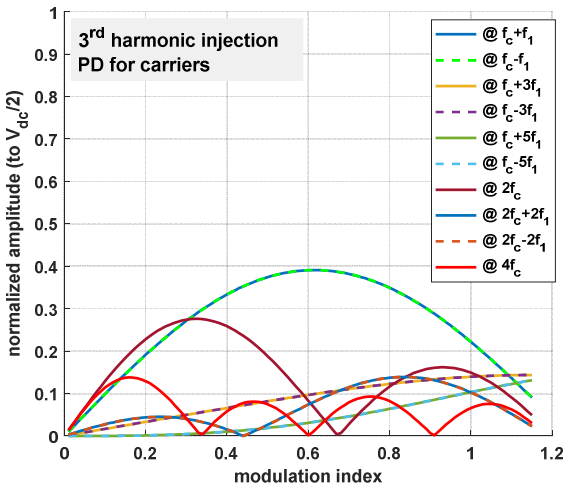


Fig. 3: Absolute switching function harmonics for PD.

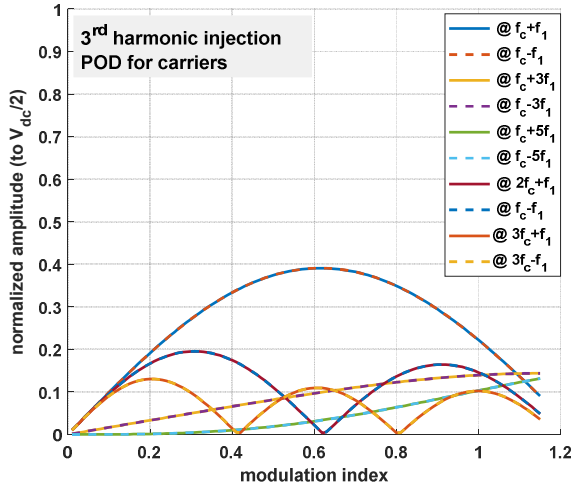


Fig. 4: Switching function harmonics for POD.

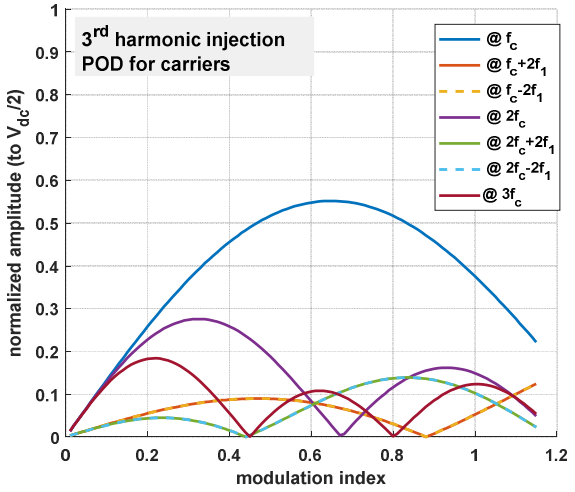


Fig. 5: Absolute switching function harmonics for POD.

It can be observed in (12) that harmonic components are present at multiples of the carrier frequency. This is exactly the feature that gives PD its superior performance when it comes to current ripple, since the above harmonics are common-mode (CM) harmonics and do not appear in the line-to-line or the phase-to-star point voltage. In addition, one can observe odd sidebands around even carrier multiples and even sidebands around odd carrier multiples. As with all CB-PWM strategies, the triplen sideband harmonics (i.e. multiples of three of the fundamental) are CM harmonics and cancel in the line-to-line voltage [5].

The absolute value of the switching function can be expressed as the following sum of harmonics:

$$|u_a| = \sum_{m\epsilon\mathbb{N}} \frac{1}{2m} C_{2m} \sin[2m\omega_c t] + \sum_{m\epsilon\mathbb{N}} \frac{1}{2m-1} \sum_{n\epsilon\mathbb{Z}} C_{2m-1,2n+1} \sin[(2m-1)\omega_c t + (2n+1)\omega_1 t] + \sum_{m\epsilon\mathbb{N}} \frac{1}{2m} \sum_{n\epsilon\mathbb{Z}\setminus\{0\}} C_{2m,2n} \sin[2m\omega_c t + 2n\omega_1 t]. \quad (14)$$

In the case of POD the switching function can be expressed as the following sum of harmonics:

$$u_a = \frac{2}{\pi} \sum_{m\epsilon\mathbb{N}} \frac{1}{m} \sum_{n\epsilon\mathbb{Z}} C_{m,2n+1} \cos[m\omega_c t + (2n+1)\omega_1 t]. \quad (15)$$

The absolute value of the switching function can be expressed as the following sum of harmonics:

$$|u_{\mathrm{a}}| = \sum_{m\epsilon\mathbb{N}} \frac{1}{m} \sum_{n\epsilon\mathbb{Z}} \mathrm{C}_{m,2n+1} \sin[m\omega_c t + (2n+1)\omega_1 t]. \quad (16)$$

Consider CB-PWM with a sinusoidal CM component at three times the fundamental frequency that extends the linear region of the modulator. This technique is known as "third harmonic injection" [5]. Numerical analysis via FFT shows in the case of PD a strong CM harmonic component in the switching function at the switching frequency (cf. Fig. 2), which takes its maximum value close to a modulation index of $m_{3\mathrm{L}} \approx 0.65$. This component does not appear in the harmonics of the absolute value of the switching function (cf. Fig. 3). When POD is applied the opposite happens: the large CM harmonic components appear only in the harmonics of the absolute value of the switching function (cf. Fig. 4 and Fig. 5).

The presence or lack of a CM harmonic component at the carrier frequency is of paramount importance for the amplitude of the NP potential ripple and of the total dc-link ripple, as it will become clear from the harmonic transfer rules and the numerical analysis presented in the next sections.

## Harmonics transfer rules from the ac to the dc side

As shown in the previous section the total dc-link voltage and the NP potential can be calculated from the convolution of the phase currents with the switching functions and their absolute value respectively. In such calculations sums of the three-phase quantities appear. In [4] symmetrical operating conditions were assumed and the following rules have been derived for the resulting dc-link components in the frequency domain:

1. If the symmetrical components of the current harmonic and the switching function harmonic describe either a positive-sequence system or a negative sequence system, then their convolution onto the DC side will result in a single harmonic.

2. If the current harmonic and the switching function harmonic have the same/different phase sequence, the harmonic order of the resulting dc-link harmonics will be the difference/sum of the individual AC-side harmonic orders.

3. If the symmetrical components of either the current harmonic or the switching function harmonic describe a zero-sequence system, their convolution will not result in any dc-link harmonics.

The above harmonic transfer rules, especially the last one, are very important for the understanding of the results that are presented in the next section. They show that only some sums and differences of frequencies appear in the dc-link harmonic components whereas others cancel out when the sum of the three phases is considered.

## Harmonics of the dc-link voltage ripple

Consider a 3.3 kV converter rated at 8.5 MVA with a total dc-link voltage of 5 kV for a WECS. Characteristic numerical results for the harmonics of the NP potential, total dc-link voltage and upper (dc-link) capacitor voltage are presented in Fig. 6 - Fig. 7, Fig. 8 - Fig. 9, and Fig. 10-Fig. 11 respectively. Naturally sampled CB-PWM has been considered. The selected carrier frequency $\mathrm{f_c} = 350$ Hz for the investigation lies in the range of typical carrier frequencies of converters in this power range; the fundamental frequency (of the generator) is $\mathrm{f_1} = 10$ Hz. The current ripple has been neglected in the analysis, since it is very small for such a carrier to fundamental frequency ratio. The CB-PWM reference includes a CM component of three times the fundamental frequency that extends the linear region of the modulator.

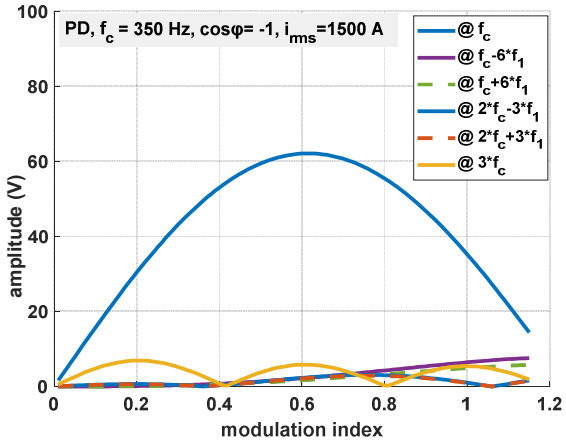


Fig. 6: Harmonics of the NP potential for PD.

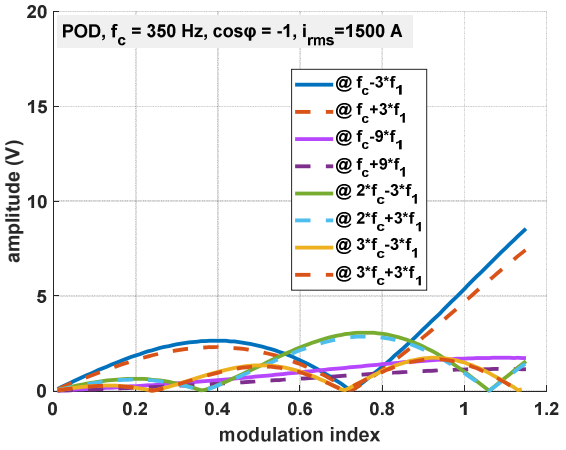


Fig. 7: Harmonics of the NP potential for POD.

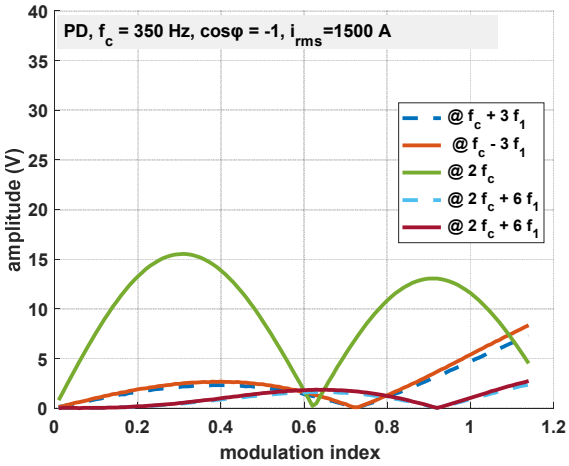


Fig. 8: Harmonics of the total dc-link voltage for PD.

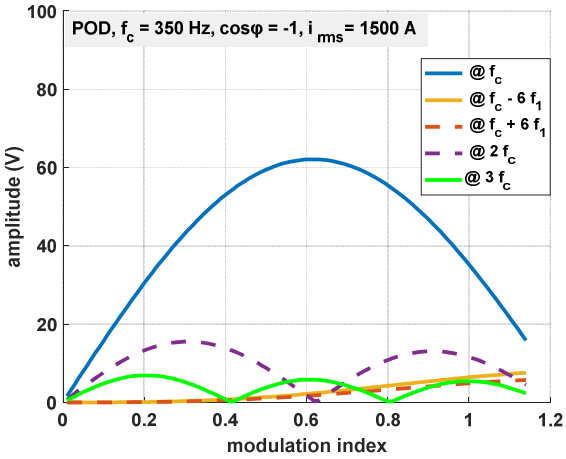


Fig. 9: Harmonics of the total dc-link voltage for POD.

In Fig. 6 - Fig. 7 one can observe that if PD is used a strong harmonic component at the carrier frequency is present in the NP potential, which doesn't appear when POD is employed. This happens because in POD a strong CM component at the carrier frequency appears in the absolute value of the switching function (cf. Fig. 5). The latter does not cause any component on the dc-side according to the harmonic transfer rule No. 3 of the previous section. The strongest harmonic components of the NP ripple in the case of POD appear at $f_c \pm 3f_1$ and at $f_c \pm 9f_1$. Their amplitudes are significantly smaller than those at the carrier frequency in the case of PD.

Regarding the harmonics on the total dc-link voltage, it can be clearly seen that PD produces lower harmonics compared to POD (cf. Fig. 8 and Fig. 9). In POD a strong harmonic component at the carrier frequency appears, whose amplitude gets its maximum value for a modulation index of approximately 0.62. Because of this strong harmonic component POD is suboptimal when it comes to dc-link voltage ripple. In PD no strong component close to the carrier frequency appears, because the harmonic of the switching function at the carrier frequency is a CM harmonic (see again rule No. 3 of previous section).

For the semiconductors the sum or the difference of the previously discussed quantities is critical, i.e., the voltage harmonics of the upper (or lower) dc-link capacitor. This voltage contains the harmonics from both the NP potential and the total dc-link voltage. Because of that the voltage harmonics have the same frequency and amplitude regardless of the selection of PD or POD. An inspection of Fig. 10 and Fig. 11 proves that. In fact, for all possible phase displacements between the two carriers the frequencies and the amplitudes of the harmonics are the same.

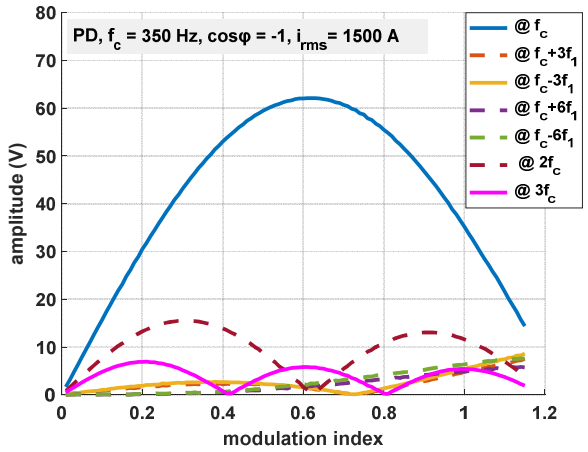


Fig. 10:Harmonics of the upper half of the dc-link voltage for PD.

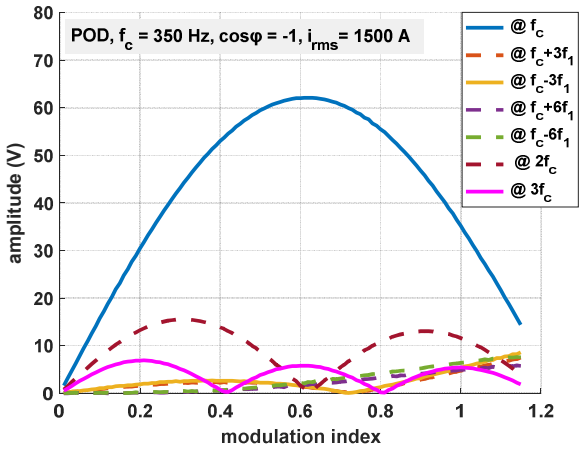


Fig. 11: Harmonics of the upper half of the dc-link voltage for POD.

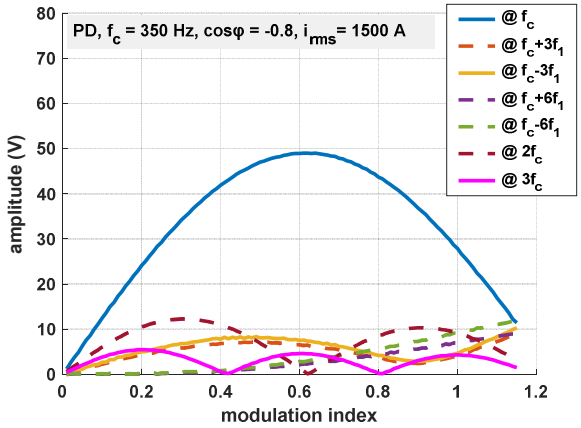


Fig. 12: Harmonics of the upper half of the dc-link voltage for PD.

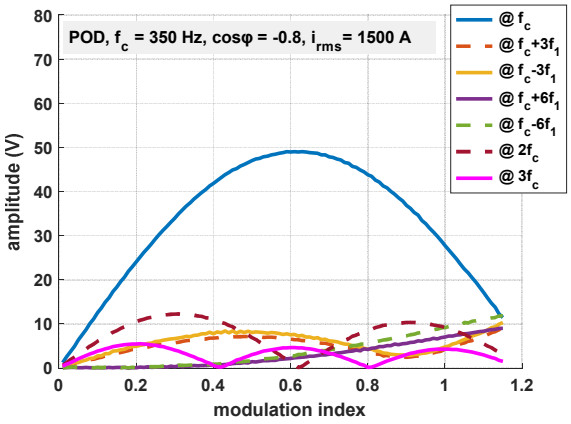


Fig. 13: Harmonics of the upper half of the dc-link voltage for POD.

For a given carrier frequency and dc-link capacitance their amplitudes depend only on the current displacement factor. Their amplitudes decrease slightly with decreasing displacement factor as can be seen when comparing Fig. 12 with Fig. 13.

## Conclusion

The switching related ripple of the dc-link voltage of a carrier-based pulse width modulated three-level converter has been investigated. Of special interest is the voltage ripple of each half of the dc-link. Its peak value must not exceed the maximum blocking voltage of the semiconductors. Numerical analysis has shown that although the harmonics of the NP potential and the harmonics of the total dc-link voltage depend on the relative phase of the two carriers, the harmonics of the upper and the lower half of the dc-link voltage are unaffected by the carrier phase. For a given carrier frequency and dc-link capacitance their amplitudes are influenced only be the displacement factor of the fundamental current component.

The presented analysis is valid for high ratios between the carrier frequency and the fundamental frequency, as it is the case for gearless wind energy generation systems. In such a case the current ripple doesn't contribute significantly to the dc-link voltage ripple and can be neglected.

# References


[1] Ogasawara S. and Akagi H., Analysis of variation of neutral point potential in neutral-point-clamped voltage source PWM inverters, IEEJ Transactions on Industry Applications, November 1993, pp. 965-970.

[2] Song Q., Lui W., Yu Q. and Wang X., A neutral-point potential balancing algorithm for three-level NPC inverters using analytically injected zero-sequence voltage, 18th Annual IEEE Applied Power Electronics Conference and Exposition (APEC), February 2003, pp. 228-233.

[3] Wang Ch. and Li Y., Analysis and calculation of zero-sequence voltage considering neutral-point potential balancing in three-level NPC converters, IEEE Transactions on Industrial Electronics, July 2010, pp. 2262-2271.

[4] Scheuer G., Investigation of the 3-level voltage source inverter for flexible AC transmission systems exemplified on a static VAr compensator, Dissertation, ETH Zurich 1997.

[5] Holmes D.G. and Lipo T.A, Pulse width modulation for power converters, IEEE Press, 2003.